HHS Public Access

Author manuscript

Cytometry A. Author manuscript; available in PMC 2022 June 13.

Published in final edited form as:

Cytometry A. 2008 May ; 73(5): 400–410. doi:10.1002/cyto.a.20555.

Nine-Color Flow Cytometry for Accurate Measurement of T Cell Subsets and Cytokine Responses. Part I: Panel Design by an Empiric Approach

Bridget E. McLaughlin[1], **Nicole Baumgarth**[2], **Martin Bigos**[3], **Mario Roederer**[4], **Stephen C. De Rosa**[5], **John D. Altman**[6], **Douglas F. Nixon**[7], **Janet Ottinger**[8], **Carol Oxford**[9], **Thomas G. Evans**[10], **David M. Asmuth**[1,*]

[1]Division of Infectious Diseases, Internal Medicine, University of California Davis, Davis, California

[2]Center for Comparative Medicine, University of California Davis, Davis, California

[3]Gladstone Institute of Virology and Immunology, San Francisco, California

[4]National Institutes of Health (NIH), NIAID, Bethesda, Maryland

[5]Fred Hutchinson Cancer Research Center, University of Washington, Seattle, Washington

[6]Emory Vaccine Center at Yerkes, Emory University, Atlanta, Georgia

[7]Division of Experimental Medicine, University of California, San Francisco, California

[8]Duke Center for AIDS Research, Duke University Medical Center, Durham, North Carolina

[9]Medical Pathology and Laboratory Medicine, University of California Davis, Davis, California

[10]Novartis Institute of Biological Research, Cambridge, Massachusetts

Abstract

Polychromatic flow cytometry offers the unprecedented ability to investigate multiple antigens per cell. Unfortunately, unwanted spectral overlaps and compensation problems increase when more than four colors are used, but these problems can be minimized if staining combinations are chosen carefully. We used an empiric approach to design, test and identify six-color T cell immunophenotyping reagent panels that can be expanded to include three or more functional or other markers in the FITC, PE, and APC channels without significant spectral limitations. Thirty different six-color T cell surface antigen reagent panels were constructed to identify major T cell subsets and maturational subtypes as defined by CCR7 and CD45RA expression, while excluding monocytes, B and non-viable cells. Staining performance of each panel was compared on cryopreserved cells from a single healthy donor recorded on a multiparameter cell sorter. Ten of the thirty reagent panels offered reliable resolution of T cell major and maturational surface markers. Of these, two panels were selected that showed the least spectral overlap and resulting background increase in the FITC, PE, and APC channels. These channels were left unoccupied for inclusion of additional phenotypic or functional markers, such as cytokines. Careful reagent

*Correspondence to: David M. Asmuth, University of California-Davis Medical Center, Division of Infectious Diseases, 4150 V Street, PSSB G500, Sacramento, CA 95817-1460, USA. david.asmuth@ucdmc.ucdavis.edu.

titration and testing of multiple candidate panels are necessary to ensure quality results in multiparametric measurements

Keywords

polychromatic flow cytometry; T cell immunophenotyping; fluorochrome conjugated antibody; compensation

Polychromatic flow cytometry allows for detailed measurements even with small sample sizes and has recently been advanced by the development of new instrumentation, reagents and data analysis tools. Despite these significant improvements, it can be difficult to derive meaningful results when reagent combinations are expanded to include eight or more fluorescent markers. This is because unwanted spectral overlaps and measurement errors worsen as the number of fluorochromes used to label coordinately expressed cell markers increase (1-3). Using appropriate controls, software compensation algorithms can correct spillover problems post acquisition. However, due to the increased number of spectral overlaps in polychromatic reagent combinations, even properly compensated data can exhibit unwanted spreading into other measurement channels, complicating data analysis and interpretation (3,4). For example, dimly expressed markers, such as cytokines, are difficult to measure in channels where spreading in properly compensated data increases the background in the cytokine measurement channel. Such data spread in effect masks low intensity events; a problem not usually apparent when only a few stains are used simultaneously.

A variety of sources contribute to this error in compensated data and are partially corrected by newer digital electronic configurations that collect and store data on a linear scale (2,3). However, photon counting error is a function of the fluorescent emission of each dye and will contribute error to compensation calculations regardless of instrument design (2,3). Counting errors are influenced by signal intensity and the degree of spillover, and are minimized by using bright dyes with as little spectral overlap as possible. While relative dye brightness (4) and spectral overlaps can be predicted (5), these factors are also influenced by the density of antigen expression. Thus, the counting errors generated by particular antibody and fluorochrome combinations may promote a high degree of spreading into spillover channels, limiting the usefulness of certain reagent combinations. Unfortunately, these effects are difficult to predict and pose a significant hurdle to the design of optimal polychromatic reagent panels. In this manuscript, we describe an empiric approach to clearing this hurdle in the setting of intracellular cytokine expression within T cell maturational subsets, while providing insights that can be applied to the design of any multicolor panel.

In the final analysis, a useful polychromatic reagent panel can best be developed by an empiric exercise of methodically testing the desired antibody panel with as many permutations of antibody-fluorochrome combinations as possible. The drawback to this approach is that testing multiple reagent combinations is time-consuming and expensive. A simpler strategy is to break the full panel into smaller subsets and to focus on optimizing a group of necessary markers before including additional stains. To illustrate this process,

we describe our efforts to design a 9-color reagent panel to enumerate vaccine-responsive memory and effector T cells in multicenter clinical trials. We began by ranking our panel constituents based on predicted expression levels, reserving the "brightest" fluorochromes for the eventual measurement of three cytokines, IFNγ APC, IL-2 PE, and TNFα FITC. Then, using antibodies conjugated to "duller" stains, we tested thirty permutations of six-color T cell surface antigen "anchor" panels to identify reagent combinations that maximized the measurement of T cell phenotypes while maintaining sensitivity in cytokine channels.

Materials and Methods

Cell Isolation and Stimulation

Six-color T cell surface antigen panels were tested using peripheral blood mononuclear cells (PBMC) from a single, healthy volunteer. PBMCs were isolated from leukocyte-enriched whole blood by Ficoll density separation (Histopaque-1077, Sigma-Aldrich, St. Louis, MO) and immediately cryopreserved in 90% FBS (Omega Scientific) with 10% DMSO (Sigma Aldrich). For each experiment, cryopreserved PBMCs were reconstituted with pre-warmed 20% RPMI + supplements (Sodium pyruvate [1mM], HEPES [10mM], NEAA [1X], L-Glutamine [2mM], Penicillin-Streptomycin [100 u/mL–100 μg/mL), treated with 50 units (5 μl of 10 U/μl) of DNase 1 (RNase-free, Roche Applied Science, Indianapolis, IN) for 5 min at 37°C water bath to digest extracellular DNA and reduce cellular clumping, washed and resuspended in 20% RPMI, and allowed to rest in culture overnight at 37°C. In all experiments, ~2 × 10^6 rested cells/mL were stimulated for 6 h at 37°C with Staphylococcus enterotoxin B (SEB) (5 μg/mL, Sigma-Aldrich) + anti-CD28 (1 μg/mL, BD) + anti-CD49d (1 μg/mL, BD) in the presence of brefeldin A (10 μg/mL, Sigma). Stimulated cells were stored at 4°C for convenience and stained the following day.

Cell Staining

Activated cells were washed in cold buffer (1× PBS with 1% bovine serum albumin [BSA]), pelleted and surfacestained for CD4, CD8, CD14, CD19, CD45RA, and CCR7 antigens in the presence of 0.5 μg/mL ethidium monoazide (EMA, Molecular Probes, Eugene, OR) for 15 min at room temperature in the dark. All samples were exposed (15 min) to a bright white light source to photochemically crosslink EMA within the nucleic acids of nonviable cells. This brief light exposure did not affect fluorochrome performance (data not shown). Unincorporated EMA and surface antibodies were washed away prior to fixation (BD Cytofix/Cytoperm kit, BD Biosciences) and subsequent intracytoplasmic staining for CD3 in saponin buffer (BD Perm/Wash, BD Biosciences). After two washes in BD Perm/Wash and a final PBS/BSA wash, the cells were resuspended in PBS/BSA with 0.5% paraformaldehyde and analyzed immediately or stored at in the dark at 4°C for a maximum of 24 h prior to flow cytometric analysis.

Initial Testing and Titration of Monoclonal Antibody Fluorochrome Conjugates

The monoclonal antibodies used in all panels were individually tested as surface or intracytoplasmic stains on SEB stimulated PBMCs to determine staining performance and optimal dilutions for each reagent (Table 1). Optimal antibody dilutions were determined for

each monoclonal antibody by staining 2×10^5 PBMC from a healthy donor with two-fold dilutions of antibody ranging from 1:5 to 1:5,000. Surface antibodies were added to cells in a total volume of 50 μl of cold 1× PBS with 1% BSA for 20 min, washed once, fixed in 4% paraformaldehyde for 20 min at room temperature (BD Cytofix/Cytoperm kit, BD Biosciences), washed and resuspended in 1X PBS with 0.5% paraformaldehyde (Sigma). Intracytoplasmic stains were added to fixed PBMCs (20 minutes, room temperature, BD Cytofix/Cytoperm kit, BD Biosciences) in a total volume of 100 μl of cold saponin buffer (BD Perm Wash) for 20 min, washed twice in Perm Wash and resuspended in 1× PBS with 0.5% paraformaldehyde. A pretitrated CD3 stain was included with all CD4, CD8, CD45RA, and CCR7 titrations to identify T cells. Following immediate flow cytometric analysis (20,000 events collected per sample), a ratio of the positive/negative median fluorescent intensity was computed for each dilution. The dilution that resulted in the largest separation between stained cells and unstained (negative) background (highest ratio) was chosen for use in each staining panel.

Since T cell receptor (TCR) triggering by super-antigen or cognate antigen induces down-regulation of the TCR (6), it was important to use an anti-CD3 monoclonal antibody whose affinity for internalized CD3 molecules was unaffected by fixation and intracellular staining conditions. The UCHT-1 clone demonstrated consistent intracytoplasmic staining performance and was therefore used exclusively in all the staining panels. All of the other T cell antigens in the six-color staining panels performed best under surface staining conditions. The listed CD3, CD4, and CD8 reagents used in comparing the thirty anchor panels, as well as many other test antibody samples (data not shown), were generously donated by Beckman Coulter, Becton-Dickinson, and Caltag Laboratories.

Data Acquisition and Analysis

All flow cytometric data were acquired using a modified Cytomation MoFlo jet-in-air cell sorter, equipped with analog pulse processing electronics and customized emission optics to detect 11 individual fluorescent signals excited by 150 mW 407 nm krypton violet, 200 mW 488 nm blue and 200 mW 647 nm red lasers (7). Instrument performance was verified before acquisition using standard fluorescent microparticles (SPHERO Rainbow Fluorescent Particles, RFP 30–5A, Spherotech, IL). A single 612/25 bandpass filter was used to collect the light from the PE-Texas Red, ECD and PE-Alexa 610 stains. Despite the absence of cytokine stains in these analyses, the FITC, PE, and APC detectors were set to voltages typically used for surface stain measurements to assess the amount of background expansion in these channels. Uncompensated data were collected for all experiments. Compensation corrections were computed and all analyses were carried out using FlowJo (Tree Star Inc, Ashland, OR). Bivariate histograms are displayed using compensated data with 0 and negative log scaling (8). For each 6-color anchor panel, 100,000 total events were collected and gated to identify lymphocytes (FSC vs. SSC), exclude dump positive cells (EMA, CD14 and CD19 PE-Cy5), identify CD31 T cells, subdivide CD31 T cells into CD4 and CD8 T cell subsets, and define CD41 and CD81 maturational subtypes based on CCR7 and CD45RA expression patterns.

Results

Panel Design Strategy

The goal of these studies was to develop a 9-color reagent panel to enumerate vaccine-responsive T cells in multicenter clinical trials. Applying a stepwise approach to panel design, we tested multiple permutations of six-color T cell surface-antigen “anchor” panels that could be supplemented with additional functional or phenotypic stains to suit individual clinical protocols. Vaccine-induced T cell cytokine responses are very rare (<1% of CD4 or CD8 T cells), therefore we used SEB superantigen stimulation to generate a readily measurable T cell response by which to compare reagent panel performance and to approximate the conditions to be used in future antigen-specific assays (9).

Several rules guided the development of candidate 9-color panels, including our knowledge of the expression level of each antigen on activated T cells, the relative brightness of each dye, and the amount of spectral overlap each dye contributes to or receives from other fluorochromes. On the basis of practical limitations such as instrument optical configuration and commercial reagent availability, we chose from the following fluorochromes to construct our panels: Pacific Blue, Quantum-Dot 655, FITC, PE, PE-Texas Red (or ECD or PE-Alexa 610), PE-Cy5, PE-Cy7, APC, Alexa 700 and APC-Alexa 750. Of these, PE, APC, and FITC were reserved as channels that could be used to detect the expression of dimly-fluorescent markers, such as cytokines, which are generally only available in limited conjugated products.

CD45RA and chemokine receptor seven (CCR7) stains were included to further subdivide $CD4^+$ and $CD8^+$ T cells into maturational subsets, defined as: naïve (N) $CCR7^+$, $CD45RA^+$; central memory $CCR7^+$, $CD45RA^-$; effector memory $CCR7^-$, $CD45RA^-$; and RA^+ memory $CCR7^-$, $CD45RA^+$ (10,11). Certain CD45RA conjugates exhibited reduced staining intensity post-fixation for reasons that are not clear (data not shown). CD45RA (clone MEM56) conjugated to Qdot 655 resulted in the best separation of positive populations over background under intracellular staining conditions (Fig. 1). Further testing also confirmed the superior performance of the PE-Cy7 CCR7 conjugate, and therefore CD45RA QD655 and CCR7 Cy7PE stains were used in all 30 candidate panels.

A set of negative selection markers detected in a single fluorescence channel, which we refer to as the ‘dump channel’, were included to reduce unwanted nonspecific antibody binding when measuring rare populations. The negative selection markers excluded dead cells, B cells and monocytes from subsequent gating decisions (1,5). Dead cells were labeled with EMA, a membrane impermeant dye that is compatible with the fixation and permeabilization steps required for the intracytoplasmic detection of accumulated cytokines (12).

We used four fluorochromes, Pacific Blue, PE-Texas Red (and similar), Alexa 700 and APC Alexa 750, to detect CD3, CD4, and CD8 antigens since 1) these markers are expressed at high levels on T cells, 2) a variety of antibody clones and fluorescent conjugates of these dyes are commercially available, and 3) these antigens exhibit distinct positive versus negative staining patterns and are usually well resolved, even with dimmer stains or dyes

that receive a high degree of spectral spillover. When these strongly expressed markers are paired with dyes that have broad emission spectra, they may contribute excessive background spreading and decrease measurement sensitivity in other detection channels (13-15). Considering these factors, we acquired a large number of CD3, CD4, and CD8 antigens conjugated to these fluorochromes and tested multiple permutations of each (Table 2) to identify combinations that optimized the measurement T cell lineages while limiting background spread into the channels reserved for cytokine measurement.

Identification of Lineage Marker Conjugates

Each anchor panel was tested using reconstituted cells from a single donor. The results were compared in order to identify reagent combinations that optimized the measurement of CD3, CD4, and CD8 T cell lineages, based on prior scatter gating and exclusion of "dump positive" cells. $CD4^+$ and $CD8^+$ cells were poorly defined in twenty of the candidate reagent combinations, as shown in Figure 2 for selected panels. The $CD4^+$ subset was well defined in panels 15 and 16 (CD4 PE-TR or PE-Alexa 610, respectively), but the CD8 Pacific Blue subset was broad and appeared to overestimate a $CD4^{dim}$CD8+ population. In contrast, when the same CD4 stains were used in combination with CD8 APC-Alexa 750, as in panels 18 and 19, $CD8^+$ populations are indistinct. Finally, in panels 17, 20, 21, and 22, the CD4 APC-Alexa 750 reagent was dim and did not clearly define $CD4^+$ cells when used in combination with CD8 Pacific Blue or PE-Texas Red (or similar) stains. Note that panels 6, 8, and 10 included a CD3 Pacific Blue reagent, whereas panels 15–22 contained CD3 Alexa 700.

Refinement of Reagent Selections

Reproducibility.—From this first round of testing, 10 panels were identified that reliably identified CD3, CD4 and CD8 T cells, specifically panels: 11, 12, 14, 23, 24, 26, 27, 28, 29, and 30. These panels were chosen for replicate analysis on a single occasion using SEB stimulated PBMCs from the same blood donor used in the initial comparisons. Three fluorescence minus one (FMO) controls were included to assist in gating out 'dump' positive cells and to accurately define maturational subsets (Fig. 3) (1,5,14). FMO controls for each panel included: 1) all stains except for the combined dump stains, 2) all stains except for CD45RA QD655, and 3) all stains except for CCR7 Cy7PE. Estimates of $CD8^+$ T cell frequency were more consistent (CV 3.7%) than $CD4^+$ subsets (CV 4.7%), but the measurement of CD4 and CD8 memory populations varied depending on the staining combination used (Table 3, CV range 5.7%–24.6%). Results were evaluated to identify panels that optimized the measurement of single positive $CD4^+CD8^-$ and $CD4^-$ $CD8^+$ T cells and minimized background spreading into the FITC, PE, and APC channels reserved for cytokine measurement.

Staining quality.—Reliable resolution of $CD3^+/CD4^+$ and $CD3^+/CD8^+$ populations was achieved with all of the 'top ten' panels. Four of the 10 panels that met minimum acceptance standards overestimated regions of double positive (DP) $CD4^+CD8^+$ T cells for reasons that are unclear (Fig. 4). In healthy individuals, the percentage of $CD4^+CD8^{low}$ DP T cells in peripheral blood typically is in the 3%–6% range, although higher frequencies have been reported in normal subjects and in mitogen-activated samples *in vitro* (16-18). Reagent

combinations that included Pacific Blue or Alexa 700 conjugates of anti-CD8 (clone OKT8) antibodies (panels 23, 26, 27, and 30) identified a higher frequency of $CD4^+CD8^+$ DP T cells than the other six panels (~9.6% vs. ~6%). Because regions of single positive CD4 and CD8 T cells could be drawn with greater confidence in panels 11–14, 24, 28, and 29, they were preferred over panels 23, 26, 27, and 30 (Fig. 4).

Staining sensitivity.—As stated in the background section, the magnitude of spillover into adjacent channels is different depending upon the makeup of the reagent panel. To compare the potential loss of sensitivity caused by background expansion in FITC, PE, and APC channels, we estimated the amount of data spread each of the top 10 panels would contribute to these channels by dividing the 95th percentile minus the median of the fluorescence of the fully stained sample by the 95th percentile minus the median fluorescence of the negative control sample as described previously (7). A ratio of one indicates no difference between the background of the fully stained and compensated sample and the amount of spread observed in the negative control sample. Figure 5A compares the relative amount of increased background per panel in the FITC, PE, and APC channels. For example, in panel 12, the spillover fluorescence ($35.2_{95\%ile}$–6.5_{median}) in the PE channel is divided by the background of the negative sample ($12_{95\%ile}$–5.3_{median}) in the PE channel, 28.7/6.7 = 4.3, demonstrating that panel 12 generates the greatest amount of background expansion in the PE channel. The PE channel was most affected by combined spillover errors in all panels, except panel 14. The amount of background expansion in the APC channel was lower than in the PE channel and virtually no background expansion was measured in the FITC channel (Fig. 5B).

Sensitivities in the PE and APC channels were significantly reduced for certain reagent combinations (Panels 12 and 29, Fig. 6A). When IFNγ, IL-2, and TNFα stains are present, as shown for panel 29 (Fig. 6B) a background expansion of 50 fluorescence units (APC and PE) or 10 fluorescence units (FITC) would preclude the detection of up to 4% of dimlypositive cytokine events. Overall, all panels exhibited some data spread in at least one cytokine channel, but this effect was smallest for panels 14 and 28 for all three measurement channels. Thus we conclude that out of 30 initial reagent panels tested, two (#14 and 28) provide useful stains for the identification of T cell subsets and the potential to add up to three functional measurement parameters.

Discussion

In contrast to standard four-color flow cytometry, polychromatic methods are complicated by the effects of multiple spectral overlaps and measurement errors (1,3,5), problems that are difficult to predict but can be overcome through methodical testing of reagents to identify optimal fluorochrome-antibody combinations. Through a detailed and extensive testing of many reagents, we show that of 30 possible reagent combinations only 10 combinations demonstrated reliable resolution of targeted T lymphocyte subpopulations and only 2 showed minimal affects on 3 additional measurement channels intentionally left open for flexible functional or phenotypic marker analysis. The results thus identify 2 useful panels for multicolor analysis of human T cell subsets and further highlight the need for careful reagent testing for use in such assays. The clinical application of

these methods is critically important while HIV preventative and therapeutic trials have met with disappointing results as of late despite robust immune responses observed using traditional assays such as single cytokine expression to antigen stimulation. New methods will be needed to identify immune predictors of vaccine response as a surrogate endpoint in preliminary clinical trials (19). One new approach was demonstrated by Precopio et al, reporting that polyfunctional T-cell responses (double and triple cytokine expression in T-cell subsets following antigen stimulation) correlated with protection (20).

In our system, PE-Texas Red/PE-Alexa 610- fluorescence negatively affected anchor panel performance. All reagent combinations that included PE-Alexa 610 demonstrated suboptimal measurement and separation of CD4 or CD8 subsets (panels 3, 4, 9, 10, 13, 16, 19, and 22, Fig. 2, data shown for panel 10, 16, 19, and 22 only). When tested individually in titration experiments, PE-Alexa 610 conjugates of CD4 and CD8 demonstrated very bright staining (data not shown), but also significant overlap into spectrally similar emission channels such as Cy5PE, Cy7PE, APC and Alexa 700. A single 612/25 nm (599.5 nm–624.5 nm) bandpass filter was used to collect light from PE-Texas Red, ECD and PE-Alexa 610. While this filter collects fluorescent signals across the peak of PE-Texas Red and ECD emission (615 nm) signals, it excludes the 628 nm peak signals of the PE-Alexa 610 dye. A different filter, for instance a 620/30 (615–635 nm), might have improved the resolution of T cell subsets in panels using PE-Alexa 610 conjugates on this cytometer (7).

Many panels that included CD8 in combination with any of the PE-Texas Red-type dyes could not resolve $CD4^+$ and $CD8^+$ subsets, likely due to strong spectral overlaps between the Cy5PE dump channel and these dyes (Fig. 2). Furthermore, the quality of CD4 APC-Alexa 750 fluorescence was acceptable, but relatively dim, even on singly-stained samples. When used in combination with other stains, as in panels 6, 8, 10, 17, 20–22 (Fig .2), APC-Alexa750 $CD4^1$ subsets often appeared as diffuse regions that were difficult to distinguish from $CD8^+$ cells, a problem that was overcome only in the context of reagent panel 26.

Useful polychromatic reagent combinations afford reliable identification of key T cell subsets and also maximize sensitivity in channels reserved for dimmer markers. To assess relative sensitivity between panels, we compared the magnitude of background expansion in the vacant FITC, PE, and APC “cytokine” channels after applying software compensation. As shown in Figure 5A, a significant increase in PE channel background was measured in virtually all of the top 10 panels. This is largely due to spectral overlap between PE, PE-Texas Red and EMA, and inefficient energy transfer in the PE-tandem dyes (PE-Texas Red, PE-Cy5 and PE-Cy7). However, since identical PE-Cy5, EMA and PE-Cy7 reagents were included in all panels, the chief source of background expansion in the PE channel were the PE-Texas Red and ECD conjugates. Significant data spread was also measured in all panels that included a CD3 ECD reagent (panels 23, 24, and 26) or CD4 ECD (panels 27–30), although data spread was minimized in panels 28 and 30. These results highlight the importance of careful reagent panel design. In our comparisons, the inclusion of PE-Texas Red (or similar) stains significantly diminished sensitivity in the PE channel.

In other polychromatic applications, spectral overlaps significantly reduced sensitivity in the APC channel (1,2,4). In our system, APC background expansion varied between panels, but

was generally lower than in the PE channel (Fig. 5A), likely reflecting differences in reagent availability, panel design and instrumentation from these earlier reports. In particular, newly available reagents, such as Alexa 700 and APC-Alexa 750 may have reduced data spread in the APC channel because direct conjugates of Alexa 700 eliminate the photontransfer problems that plague APC-Cy5.5 tandem dyes, while APC-Alexa 750 conjugates are slightly brighter than Cy7 based tandem fluorophores (21). However, using these newer fluorochromes did not completely eliminate data spread in the APC detector channel (Fig. 5A). Specifically, CD8 APC-Alexa 750 conjugates contributed considerably more error to compensated APC background (panels 14, 24, 28, 29) than CD4 APC-Alexa 750 (panel 26). Further, data spread in the APC detection channel is virtually absent in panels where Alexa 700 conjugates were used instead of APC-Alexa 750 tandem dyes (panels 11, 12, 23, 27, 30). Our results illustrate the problems described previously in resolving dim APC fluorescence when strongly expressed antigens, such as CD8, are measured with Cy7 (or Alexa 750) tandem conjugates of APC (14). This problem is avoided in panels that substitute direct conjugates of Alexa 700 for the longer-wavelength APC-Cy7 (or similar) tandem dyes.

FITC emission (~515 nm) is well-separated from other dyes that emit in longer red wavelengths; therefore background expansion in the FITC channel was minimal in nearly all of the top 10 panels. The lack of background expansion observed in this channel, as described previously (1,3) and shown in Figure 5, increases the effective “brightness” of this dye, particularly when multiple PE-tandem fluorochromes are used simultaneously.

In summary, useful and flexible reagent combinations can be identified using a stepwise, empiric approach (22). Our strategy was to divide the process into an information phase (I) and a testing/decision phase (II). First (I), rank desired markers based on predicted expression levels and fluorochromes by relative brightness and expected spectral overlap. Pair dim markers (e.g. cytokines) with bright dyes that receive little spectral overlap, markers with variable expression intensities (continuous expression patterns, e.g. CD45RA) with other bright dyes, and strongly expressed markers (bi-modal expression patterns, e.g. CD8) with dimmer dyes. Use negative markers to eliminate dead or unwanted cell types. Obtain a variety of conjugates of the variably and strongly expressed antigens. Titrate all reagents to assure optimal performance, then test (II) combinations of markers with variable expression intensities to identify a core set of reagents that offer maximal separation of these subsets. Add in strongly expressed markers and dump stains, and evaluate the staining performance and spectral overlap into channels reserved for dimmer markers. Using this approach, we show that only ten of thirty T cell anchor panels afforded reliable subset resolution and of these, sensitivity in the PE and APC channels was affected to varying degrees due to the presence of multiple spectral overlaps and inefficient energy transfer between tandem derivatives of these dyes. Considering these factors, panels 14 and 28 offered the best combination of subset resolution, sensitivity and flexibility for use in future trials. In a companion manuscript, panels 14 and 28 are expanded to include three cytokine stains and compared using three cytometers to assess bias and variability between reagent combinations and across instrument platforms (23).

Acknowledgments

The authors thank Dr. Jennifer Taylor for helpful advice, Abagail Spinner for cytometer assistance, Thomas Knight for document assistance, and the members of the Baumgarth (Lisa Coro, Virginia Doucett), and Roederer laboratories (Pratip Chattopadhyay) for help with antibody conjugations and protocols. Many of the fluorochrome-conjugated antibody reagents used in this study were kindly provided as research samples from Caltag Laboratories (Michael Olszowy, Pat Burroughs and Alison Weber), Becton Dickinson (Holden Maecker, Jerome Zawadzki and Janine Tresidder) and Beckman Coulter (Pamela Selvaraj). We also thank each of these industry representatives for technical advice and support throughout this study.

Grant sponsor:

the National Center for Research Resources, National Institutes of Health; Grant number: C06RR-12088-01; Grant sponsor: NIH; Grant number: AI051999.

Literature cited

1. Baumgarth N, Roederer M. A practical approach to multicolor flow cytometry for immunophenotyping. J Immunol Methods 2000;243:77–97. [PubMed: 10986408]
2. Bigos M, Baumgarth N, Jager GC, Herman OC, Nozaki T, Stovel RT, Parks DR, Herzenberg LA. Nine color eleven parameter immunophenotyping using three laser flow cytometry. Cytometry 1999;36:36–45. [PubMed: 10331625]
3. Roederer M. Spectral compensation for flow cytometry: Visualization artifacts, limitations, and caveats. Cytometry 2001;45:194–205. [PubMed: 11746088]
4. Roederer M, De Rosa SC, Gerstein R, Anderson M, Bigos M, Stovel R, Nozaki T, Parks D, Herzenberg L, Herzenberg L. 8 color, 10-parameter flow cytometry to elucidate complex leukocyte heterogeneity. Cytometry 1997;29:328–339. [PubMed: 9415416]
5. Perfetto SP, Chattopadhyay PK, Roederer M. Seventeen-colour flow cytometry: Unravelling the immune system. Nat Rev Immunol 2004;4:648–655. [PubMed: 15286731]
6. Geisler C. TCR trafficking in resting and stimulated T cells. Crit Rev Immunol 2004;24:67–86. [PubMed: 14995914]
7. Baumgarth N, Bigos M. Optimization of emission optics. Methods in cell biology, Vol. 75, Cytometry: New Developments, 4th ed. San Diego, CA: Academic Press; 2004. pp 3–22.
8. Parks DR, Roederer M, Moore WA. A new “Logicle” display method avoids deceptive effects of logarithmic scaling for low signals and compensated data. Cytometry Part A 2006;69:541–551.
9. De Rosa SC, Lu FX, Yu J, Perfetto SP, Falloon J, Moser S, Evans TG, Koup R, Miller CJ, Roederer M. Vaccination in humans generates broad T cell cytokine responses. J Immunol 2004;173:5372–5380. [PubMed: 15494483]
10. Lanzavecchia A, Sallusto F. Dynamics of T lymphocyte responses: Intermediates, effectors, and memory cells. Science 2000;290:92–97. [PubMed: 11021806]
11. Sallusto F, Lenig D, Forster R, Lipp M, Lanzavecchia A. Two subsets of memory T lymphocytes with distinct homing potentials and effector functions. Nature 1999;401:708–712. [PubMed: 10537110]
12. Riedy MC, Muirhead KA, Jensen CP, Stewart CC. Use of a photolabeling technique to identify nonviable cells in fixed homologous or heterologous cell populations. Cytometry 1991;12:133–139. [PubMed: 2049970]
13. Maecker HT, Trotter J. Selecting Reagents for Multicolor Flow Cytometry. Hotlines Platinum Edition 2006. Available at www.bdbiosciences.com/pdfs/newsletters/23–9059-00.pdf.
14. Maecker HT, Frey T, Nomura LE, Trotter J. Selecting fluorochrome conjugates for maximum sensitivity. Cytometry Part A 2004;62:169–173.
15. Maecker HT, Trotter J. Flow cytometry controls, instrument setup, and the determination of positivity. Cytometry Part A 2006;69:1037–1042.
16. Zuckermann FA. Extrathymic CD4/CD8 double positive T cells. Vet Immunol Immunopathol 1999;72:55–66. [PubMed: 10614493]

17. Sullivan YB, Landay AL, Zack JA, Kitchen SG, Al-Harthi L. Upregulation of CD4 on CD8+ T cells: CD4dimCD8bright T cells constitute an activated phenotype of CD8+ T cells. Immunology 2001;103:270–280. [PubMed: 11454056]

18. Parel Y, Chizzolini C. CD4+ CD8+ double positive (DP) T cells in health and disease. Autoimmun Rev 2004;3:215–220. [PubMed: 15110234]

19. Horton H, Thomas EP, Stucky JA, Frank I, Moodie Z, Huang Y, Chiu YL, McElrath MJ, De Rosa SC. Optimization and validation of an 8-color intracellular cytokine staining (ICS) assay to quantify antigen-specific T cells induced by vaccination. J Immunol Methods 2007;323:39–54. [PubMed: 17451739]

20. Precopio ML, Betts MR, Parrino J, Price DA, Gostick E, Ambrozak DR, Asher TE, Douek DC, Harari A, Pantaleo G, Bailer R, Graham BS, Roederer M, Koup RA. Immunization with vaccinia virus induces polyfunctional and phenotypically distinctive CD8(1) T cell responses. J Exp Med 2007;204:1405–1416. [PubMed: 17535971]

21. Berlier JE, Rothe A, Buller G, Bradford J, Gray DR, Filanoski BJ, Telford WG, Yue S, Liu J, Cheung CY, Chang W, Hirsch JD, Beechem JM, Haugland RP, Haugland RP. Quantitative comparison of long-wavelength Alexa Fluor dyes to Cy dyes: Fluorescence of the dyes and their bioconjugates. J Histochem Cytochem 2003;51:1699–1712. [PubMed: 14623938]

22. Mahnke YD, Roederer M. Optimizing a multicolor immunophenotyping assay. Clin Lab Med 2007;27:469–485. [PubMed: 17658403]

23. McLaughlin BE, Baumgarth N, Bigos M, Roederer M, De Rosa SC, Altman JD, Nixon DF, Ottinger J, Li J, Beckett L, Shacklett BL, Evans TG, Asmuth DM. Nine color flow cytometry for accurate measurement of T-cell subsets and cytokine responses. Part II. Panel performance across different instrument platforms. Cytometry A 2008; 73A: in press. doi: 10.1002/cyto.a.20556 (this issue).

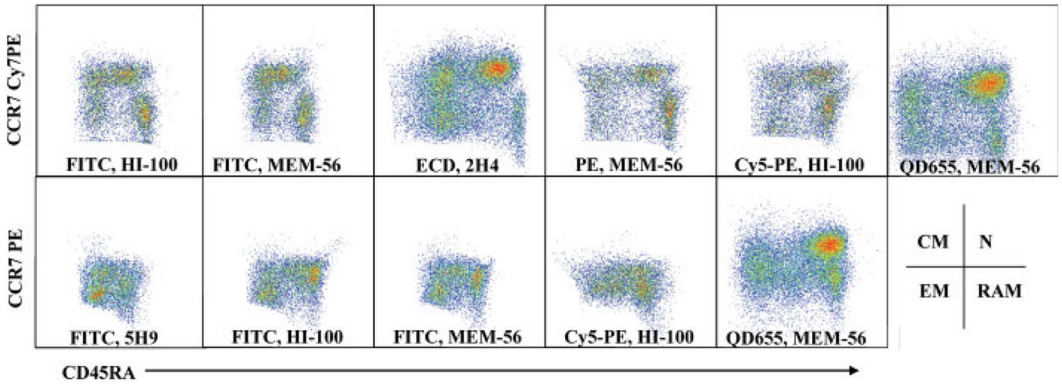

Figure 1.

Maturational marker staining combinations. Shown are pseudocolor plots of human PBMC stimulated with SEB for 6 h, gated based on forward and side scatter and expression of CD3, CD45RA, and CCR7. Shown are stains that aim to resolve the following T cell subsets: nave (N) $CCR7^{+}$, $CD45RA^{+}$; central memory (CM) $CCR7^{+}$, $CD45RA^{-}$ effector memory (EM) $CCR7^{-}$, $CD45RA^{-}$; and RA^{+} memory (RAM) $CCR7^{-}$, $CD45RA^{+}$. Pairwise combinations of PE- or Cy7PE-labeled anti-CCR7 monoclonal antibodies (vertical axes) with indicated conjugates of CD45RA (horizontal axes) were tested to identify the reagent combination that resulted in the best separation of the subsets (CCR7 Cy7PE and CD45RA QD655, upper right panel).

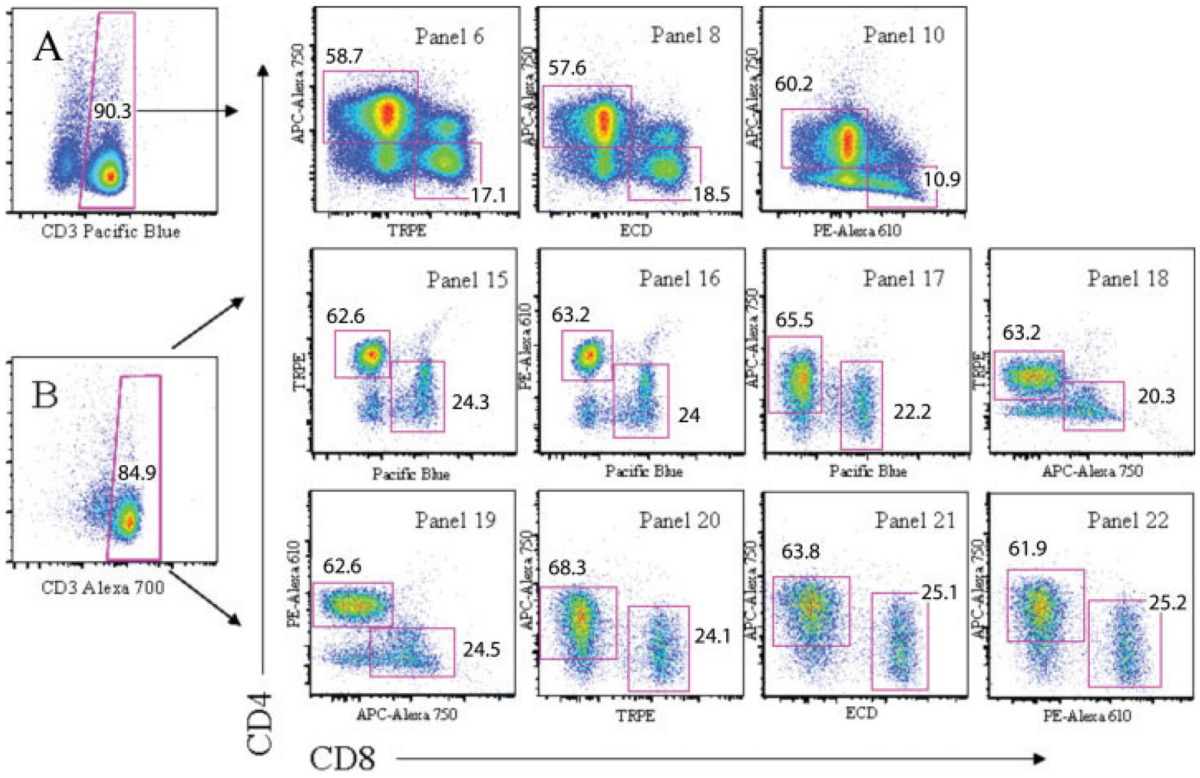

Figure 2.

Suboptimal measurement of T cell subsets with rejected staining panels. Shown are representative pseudocolor plots of PBMC stained with reagent panels that lacked sufficient separation of single positive CD4 or CD8 T cells following forward and side scatter gating, exclusion of staining for EMA, CD14, and CD19 and intracellular staining for CD3. (**A**) $CD3^+$ (Pacific Blue)/$CD8^+$ T cells are poorly defined in reagent panels 6, 8, and 10 where CD8 PE-Texas Red (or similar) reagents are combined with relatively dull CD4 APC-Alexa 750. (**B**) $CD3^+$(Alexa 700)/$CD8^+$ T cells show broad, diffuse staining patterns when used in combination with a variety of CD4 conjugates.

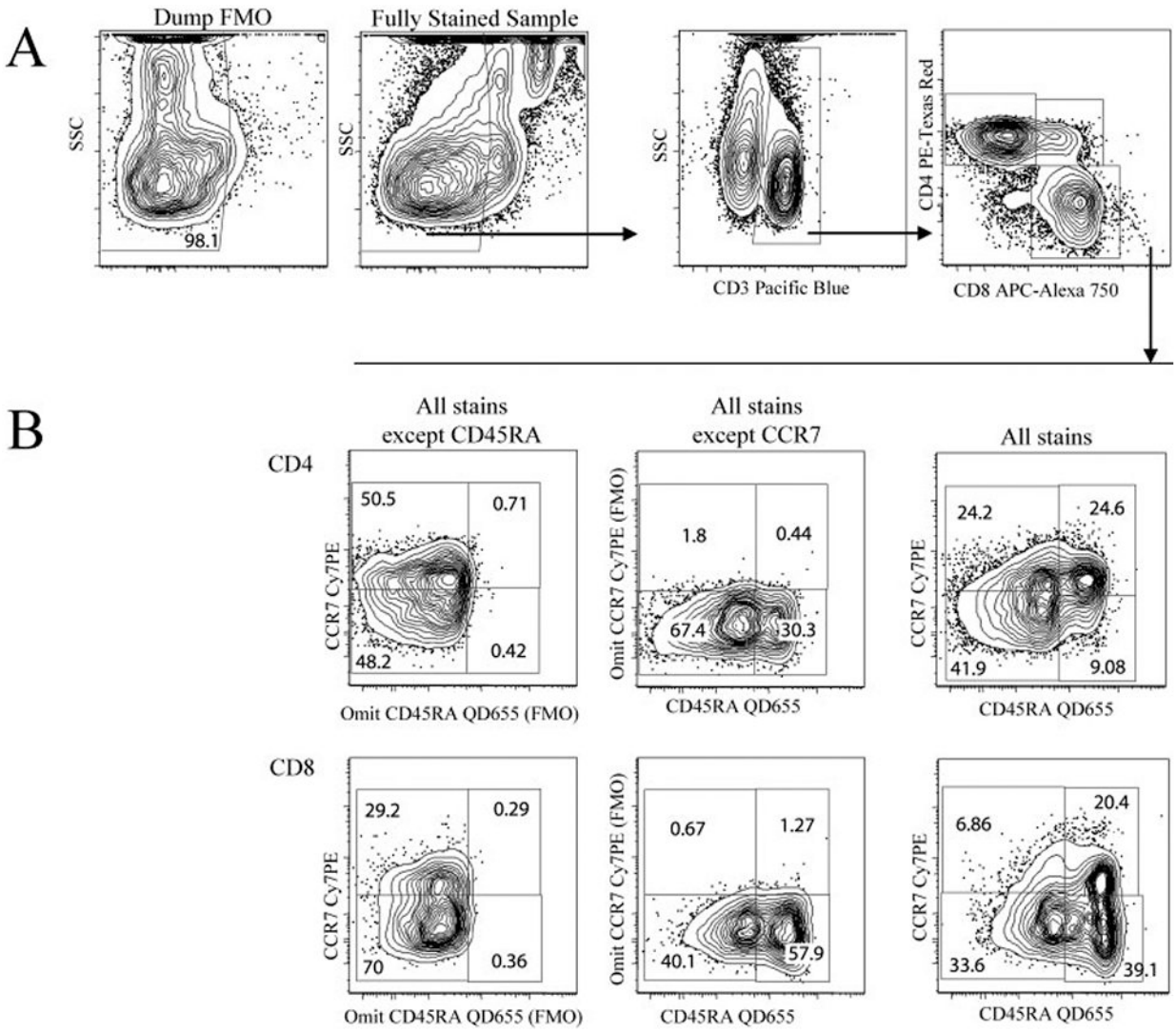

Figure 3.

Fluorescence minus one (FMO) controls. To unequivocally identify viable memory and effector T cell subpopulations, all gates were controlled using a stain that lacks just one of the fluorescent markers of interest. (**A**) Here, 5% contour plots with outliers show how a FMO control (left panel) is used to identify live cells in the fully stained sample (right panel). From there subsequent gating identifies CD3+ and then CD4 and CD8 single-stained cells. (**B**) Similarly, gating strategies to identify T cell subsets based on CD45RA and CCR7 on CD4 (top) and CD8 (bottom) staining is done comparing each stain to its respective FMO control.

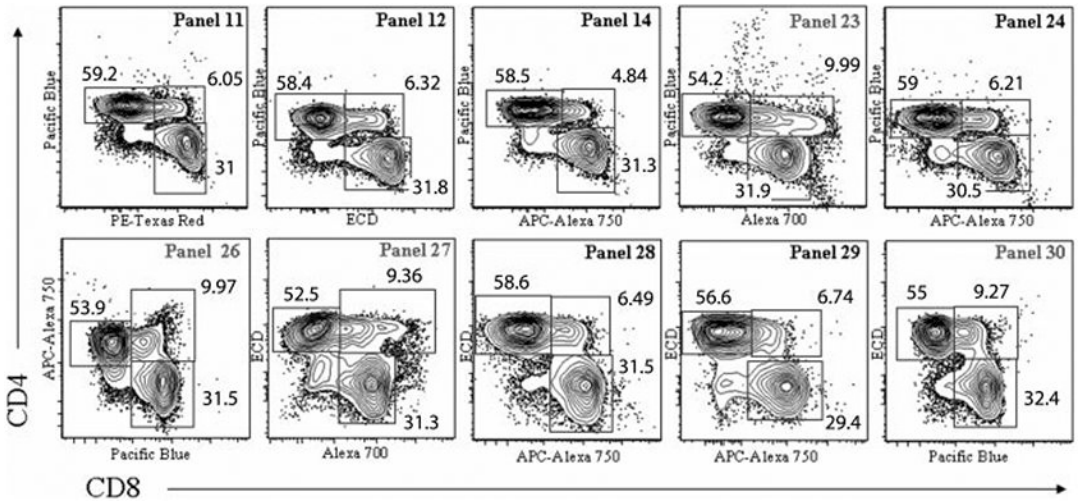

Figure 4.

Reagent panel selection. Shown are contour plots with outliers for staining of SEB-stimulated PBMC with 10 different reagent panels that afforded robust T lymphocyte subset separation. Cells were gated on lymphocyte FSC vs. SSC, exclusion of dead cells, and staining for CD3. While similar frequencies of CD4 and CD8 T cells were measured with panels 11, 12, 14, 24, 28, and 29, a higher fraction of $CD4^{+}CD8^{+}$ double positive (DP) T cells was identified in panels 23, 26, 27, and 30 (shown in red). The increased frequency of DP cells are likely due to unique and undesirable spectral interactions, or to the presence of the OKT8 CD8 monoclonal antibody, and preclude reliable measurement of $CD4^{+}$ T cells in these four panels.

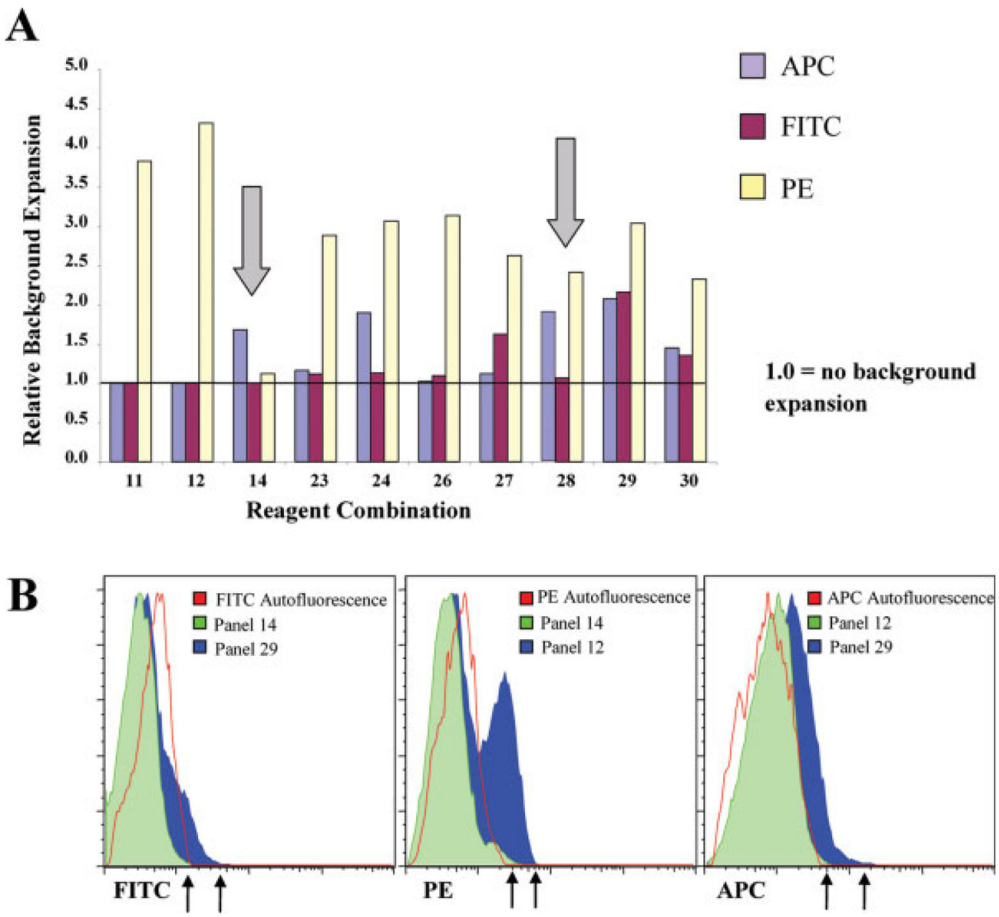

Figure 5.

Background expansion decreases sensitivity in channels reserved for cytokine measurement. Measurement errors associated with certain reagent combinations broaden the distribution of background fluorescence in fully stained samples. The increase in background of the fully stained sample, after subtracting the native background distribution of an unstained "negative" sample, is shown in (**A**) for the top 10 panels in the three channels (FITC, red bars, PE, yellow bars and APC blue bars) held vacant for functional measurements. The colored bars represent the relative amount of background expansion that results from each reagent combination, calculated as the 95%ile of the fully stained sample—50%ile of the fully stained sample/95%ile of an unstained sample—50%ile of the unstained sample. No change in background is indicted by the horizontal line. Reagent combinations 14 and 28 minimize background expansion in the FITC, PE, and APC channels (indicated by arrows), shown in (**B**). High levels of background expansion decrease sensitivity in open channels. Panels that minimized data spread (green solid histograms) are compared with the background of the unstained sample (red, open histograms) and to the reagent combination that generated the most spread (blue, solid histograms) for each cytokine channel. Red arrows indicate the position of gating cutoffs to identify positive events in panels that minimized data spread, whereas the gating cutoff would be shifted to the positions indicated by the black arrows if suboptimal reagent panels are chosen.

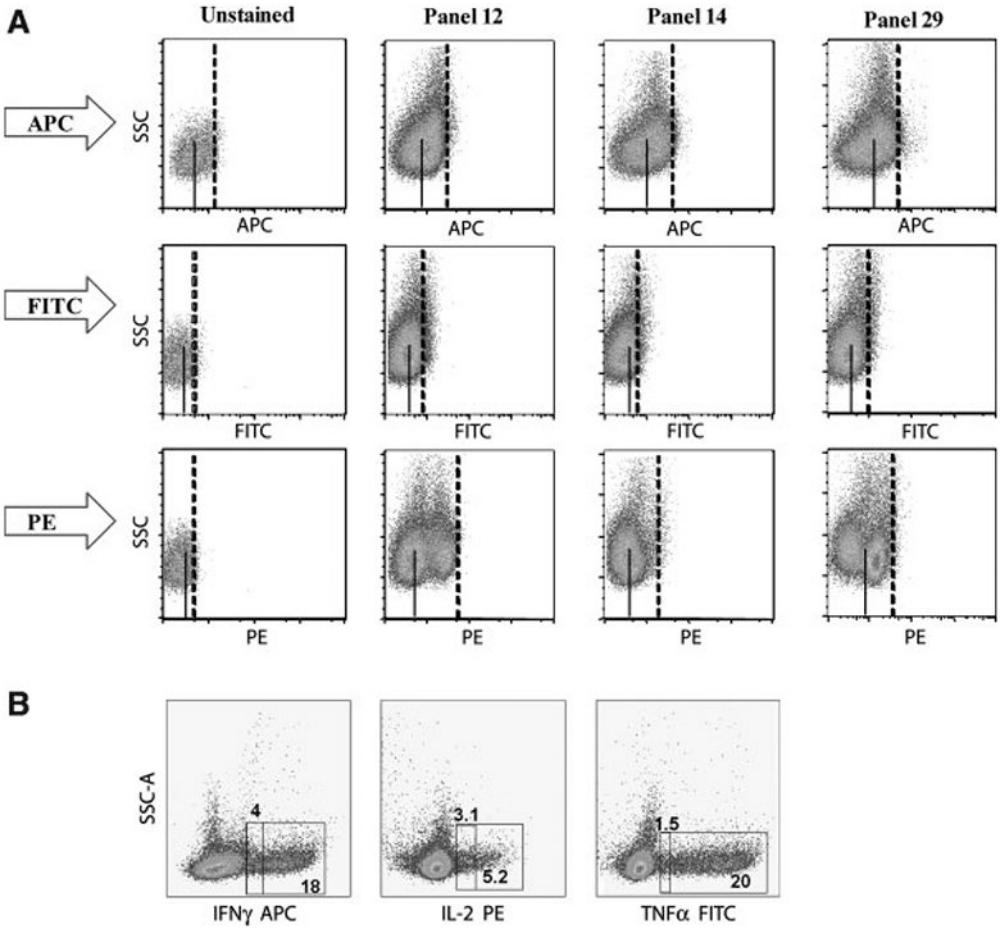

Figure 6.

Background expansion in channels held vacant for cytokine measurement. Shown in (**A**) are pseudocolor plots of cells left unstained for the measurement channel shown (APC, FITC, PE) comparing background measurements obtained when cells are stained with fluorochromes measured in other channels (panels 12, 14, and 29, Table 2). Solid lines indicate the median of the background distribution, dashed lines indicate the position of the 95th percentile of events for the FITC, PE, and APC channel and serve to illustrate the position of the negative cells. Each panel generates some increase in background, but this effect is greatest in the PE (panel 12 and 29) and APC (panel 29) channels. Panel 14 showed little increase in background staining for those channels. In (**B**) pseudocolor plots of SEB-stimulated cells (6 h with brefeldin A) stained with reagent panel 28 and for intracellular IL-2 PE, IFNγ APC, and TNFα FITC accumulation are gated to show the total percentage of cytokine producing cells (larger gate) and the percentage of cytokine expression that would be missed due to background expansion (smaller gate).

Table 1.

Reagents used in configuring thirty six-color T cell immunophenotyping reagent panels

ANTIGEN	FLUOROCHROME	CLONE	SUPPLIER	INTRACYTOPLASMIC STAINING[a]	SURFACE STAINING[a]
CD3	Alexa 700	UCHT-1	[b] BC	1:100	1:10
	Pacific Blue	UCHT-1	[c] BD	1:10	1:10
	ECD	UCHT-1		1:10	1:10
CD4	Pacific Blue	RPA-T4	BD	*	1:10
	ECD	SFC112T4D11	BC	*	1:5
	PE-Texas Red	S3.5	[d] CL	*	1:25
	PE-Alexa 610	S3.5	CL	*	1:10
	Alexa 700	RPA-T4	BD	*	1:10
	APC-Alexa 750	S3.5	CL	*	1:25
CD8	Pacific Blue	OKT8[g]	[e] IH	*	1:50
	ECD	SFC121ThyD3	BC	*	1:5
	PE-Texas Red	3B.5	CL	*	1:25
	PE-Alexa 610	3B.5	CL	*	1:25
	Alexa 700	OKT8[g]	IH	*	1:50
	APC-Alexa 750	3B.5	CL	*	1:10
CD45RA	Quantum Dot 655	MEM-56	IH	*	1:10
CCR7	PE-Cy7	3D12	BD	*	1:10
CD14	PE-Cy5	TuK4	BD	*	1:10
CD19	PE-Cy5	HIB19	BD	*	1:25
Viability	Ethidium monoazide bromide	N/A	[f] MP	N/A	1:10,000

*These reagents offered unsatisfactory signal to noise separation under intracytoplasmic staining conditions.

[a]Shown are the dilutions per 100 μl or 50 μl of staining volume for intracytoplasmic or surface staining (respectively) that produced the best signal to background ratio.

[b]Beckman Coulter.

[c]Becton Dickinson.

[d]Caltag Laboratories/Invitrogen.

[e] in house.

[f] Molecular Probes/Invitrogen Detection Technologies.

[g] ATCC CRL-8014.

Table 2.

Thirty T cell immunophenotyping anchor panels

PANEL NO.	PACIFIC BLUE	[a]PE-TEXAS RED	[a]ECD	[a]PE-ALEXA 610	ALEXA 700	APC-ALEXA 750	QD655	CY7-PE	CY5-PE
1	CD3	CD4			CD8		CD45RA	CCR7	Dump
2	CD3	CD4				CD8	CD45RA	CCR7	Dump
3	CD3			CD4	CD8		CD45RA	CCR7	Dump
4	CD3			CD4		CD8	CD45RA	CCR7	Dump
5	CD3	CD8			CD4		CD45RA	CCR7	Dump
6	CD3	CD8				CD4	CD45RA	CCR7	Dump
7	CD3		CD8		CD4		CD45RA	CCR7	Dump
8	CD3		CD8			CD4	CD45RA	CCR7	Dump
9	CD3			CD8	CD4		CD45RA	CCR7	Dump
10	CD3			CD8		CD4	CD45RA	CCR7	Dump
11	CD4	CD8			CD3		CD45RA	CCR7	Dump
12	CD4		CD8		CD3		CD45RA	CCR7	Dump
13	CD4			CD8	CD3		CD45RA	CCR7	Dump
14	CD4				CD3	CD8	CD45RA	CCR7	Dump
15	CD8	CD4			CD3		CD45RA	CCR7	Dump
16	CD8			CD4	CD3		CD45RA	CCR7	Dump
17	CD8				CD3	CD4	CD45RA	CCR7	Dump
18		CD4			CD3	CD8	CD45RA	CCR7	Dump
19				CD4	CD3	CD8	CD45RA	CCR7	Dump
20		CD8			CD3	CD4	CD45RA	CCR7	Dump
21			CD8		CD3	CD4	CD45RA	CCR7	Dump
22				CD8	CD3	CD4	CD45RA	CCR7	Dump
23	CD4		CD3		CD8		CD45RA	CCR7	Dump
24	CD4		CD3			CD8	CD45RA	CCR7	Dump
25	CD8		CD3		CD4		CD45RA	CCR7	Dump
26	CD8		CD3			CD4	CD45RA	CCR7	Dump
27	CD3		CD4		CD8		CD45RA	CCR7	Dump
28	CD3		CD4			CD8	CD45RA	CCR7	Dump

PANEL NO.	PACIFIC BLUE	[a]PE-TEXAS RED	[a]ECD	[a]PE-ALEXA 610	ALEXA 700	APC-ALEXA 750	QD655	CY7-PE	CY5-PE
29			CD4		CD3	CD8	CD45RA	CCR7	Dump
30	CD8		CD4		CD3		CD45RA	CCR7	Dump

[a]Light emitted from the three spectrally similar dyes, PE-Texas Red, ECD, and PE-Alexa 610 was measured in the same channel using a 612/25 bandpass filter.

Table 3.

T Cell subset frequencies measured with the best ten reagent combinations

PANEL NUMBER	DUMP NEGATIVE	CD3	CD4 CM	CD4 EM	CD4 N	CD4 RAM	CD4	CD8 CM	CD8 EM	CD8 N	CD8 RAM	CD8
11	75.5	70.2	59.2	29.2	31	32.1	7.61	31.1	9.46	34.7	19.9	35.9
12	71.3	68.1	58.4	25.7	35.4	31.6	7.3	31.8	8.93	30.1	22.5	38.3
14	60.5	70.8	60.6	25.4	35.9	30	8.54	30.6	6.19	33.7	18.4	41.7
23	70.2	63.1	54.1	23.4	43.1	21.5	11.9	32	7.33	32.6	19.7	40.4
24	68.3	67.8	58.9	20.4	42.9	21.6	15	30.1	7.41	28.9	22.1	41.4
26	67.7	65.7	53.9	25	41	25.2	8.87	31	7.24	36.4	15	41.3
27	71.9	67	52.8	25.8	42.7	22.2	9.28	31.7	8.91	35.2	19.6	36.2
28	67.2	68.9	56.4	24.2	41.9	24.6	9.08	30.6	6.86	33.5	20.4	39.2
29	65	53.5	58.3	27.2	40.7	23.8	8.19	28.4	6.95	33.6	23	36.5
30	67.4	62.7	55.1	26.2	39.2	26	8.58	32.3	8.66	31.3	21.5	38.4
Mean	68.5	65.8	56.8	25.3	39.4	25.9	9.4	31.0	7.8	33.0	20.2	38.9
Std. error	4.1	5.1	2.7	2.3	4.0	4.0	2.3	1.1	1.1	2.3	2.3	2.2
% CV	6.0	7.7	4.7	9.2	10.2	15.6	24.6	3.7	14.1	7.0	11.6	5.7